Data supplement for Dienel et al., The Nature of Prefrontal Cortical GABA Neuron Alterations in Schizophrenia: Markedly Lower Somatostatin and Parvalbumin Gene Expression Without Missing Neurons. Am J Psychiatry (doi: 10.1176/appi.ajp.20220676)

Supplemental Methods and Materials

Fluorescent In Situ Hybridization Tissue Labeling

For each subject, fresh-frozen coronal tissue blocks containing right DLPFC area 9 were mounted in a cryostat. Areas where the cortex had been blocked perpendicular to the pial surface were demarcated using a scalpel and sectioned with the cryostat at 20 µm thickness onto SuperFrost slides (ThermoFisher Scientific, Waltham, MA, USA), thaw-mounted, and stored at -80°C until tissue labeling. mRNA probes were designed by Advanced Cell Diagnostics, Inc (Hayward, CA, USA) to detect mRNAs encoding somatostatin (SST), parvalbumin (PV, gene symbol *PVALB*), SRY-box transcription factor 6 (SOX6), and the vesicular GABA transporter (VGAT, gene name *SLC32A1*) (**Table S2**). VGAT was used as a GABA neuron marker as it is expressed by all GABA neurons and levels of VGAT mRNA are unaltered or only modestly lower in the DLPFC of people with schizophrenia (1, 2). SOX6 (3, 4) was used to distinguish SST and PV neurons from other GABA neurons. SOX6 is selectively expressed in SST and PV neurons due to their common embryonic origin in the medial ganglionic eminence (MGE) and continues to be robustly expressed in the adult primate neocortex (5). SOX6 was favored in this experiment over other markers of MGE-derived interneurons, such as Nkx2.1, the expression of which is rapidly downregulated postnatally (5), or Lhx6, the expression of which is lower in the DLPFC in people with schizophrenia (6, 7).

Based on the study design, we employed an assay that would allow for the simultaneous fluorescent imaging of four mRNA targets together with a DAPI counterstain to label nuclei. Fluorescent *in situ* hybridization assays (RNAscope®, ACDbio, Hayward, CA, USA) version 2 (v2) kits were used to achieve four-target labeling simultaneously. Here, we use Opal fluorophores (Akoya Biosciences, Marlborough, MA, USA) in conjunction with the RNAscope v2 assay (Opal 520 – PV; Opal 570 – SST; TSA Cy 5 – VGAT). We selected our fourth fluorophore to be compatible with our existing light engine and filter sets without the need for spectral unmixing, employing the novel use of a two-step near-infrared fluorophore (Opal 780; Akoya Biosciences) to label SOX6.

Tissue sections were processed using the RNAscope® fluorescent multiplex assay v2 kits according to the manufacturer's protocol. Briefly, after removal from –80°C, tissue sections were immediately immersed in ice-cold 4% paraformaldehyde and fixed for 15 minutes, dehydrated through a series of ethanol washes (50%, 70%, 100%, and repeated 100% ethanol for 5 minutes each), followed by H_2O_2 pretreatment to quench endogenous peroxidases and reduce off-target labelling. Target probes were then hybridized to their target mRNAs for 2 hours at 40°C. After a series of amplification steps included in the assay (Amp 1-v2 for 30 minutes at 40°C, Amp 2-v2 for 30 minutes at 40°C, Amp 3-v2 for 15 minutes at 40°C), fluorophores were assigned to each target mRNA in a stepwise manner. First, horseradish-peroxidase enzymes specific to a target channel (HRP C1-C4) were applied to tissue sections for 15 minutes at 40°C. Following the addition of HRP molecules, working solutions of Opal fluorophores diluted in 1x Plus Amplification Diluent (Akoya Biosciences) were sequentially applied to tissue sections to

fluorescently target each mRNA in the following concentrations: Opal 520–1:600 (PV), Opal 570–1:750 (SST), TSA Cy5–1:600 (VGAT), and TSA-DIG–1:600 (SOX6). After each fluorophore was added, the HRP reaction was quenched using the provided HRP blocker in the V2 kit for 15 minutes at 40ºC. This process was repeated for all four targets. Opal 780, an anti-DIG antibody conjugated to the near infrared fluorophore, was diluted in PBS (1:200) and applied to the tissue section for 15 minutes at 40ºC after the last HRP block was completed, as this antibody is exquisitely sensitive to the effects of active HRP molecules.

Microscopy

Images were collected on a custom wide-field epifluorescence Olympus IX83 inverted microscope (Center Valley, PA, USA) equipped with a 6-line (350-, 405-, 488-, 568-, 647-, 750-nm) Spectra III light engine (Lumencor, Beverton, OR, USA), a high-precision XY motorized stage (Prior Scientific) with linear XYZ encoders, and a Hamamatsu ORCA-Flash 4.0 sCMOS camera. The microscope and ancillary equipment were controlled using SlideBook 6.0 (Intelligent Imaging Innovations, Inc., Denver, CO, USA) and images were captured using a 60x 1.42 N.A. oil immersion objective (Olympus).

We focus here on layers 2 and 4 for imaging as these layers are known to be differentially enriched for SST and PV neurons, respectively (8–11). Layer 2 was defined as 10-20% of the pia-white matter distance and layer 4 was defined as 40-50% of the pia-white matter distance, as previously described (12). Imaging sites were selected by taking a low magnification image (4x) of the tissue using the DAPI counterstain. A sampling grid was placed over the tissue that included the entire gray matter section,

and grids sized 110 μm x 110 μm (1024 x 1024-pixel imaging site; pixel size = 0.1075 μm/pixel) were placed 30 μm apart to avoid representation of the same cell in different sampling sites. Imaging sites that were located within the laminar zones defined above were selected for capture at 60x magnification.

Each imaging site was collected as a 3D image stack (2D images successively captured at intervals separated by 0.25 μm in the z-dimension). Our initial pilot results suggested that 14 z-planes successfully captured the full range of in-focus mRNA grain information. In total, six channels were captured. Five channels were dedicated to imaging DAPI, PV, SST, VGAT, and SOX6 (DAPI (ex 359nm, em 461nm), FITC (ex 495nm, em 519 nm), TRITC (ex 552 nm, em 578 nm), Cy5 (ex 649 nm, em 666 nm) Cy7 (ex 753nm, em 775 nm), respectively). The 6th channel (custom 495 ex/666 em filter combination, as previously described (12, 13)) was used to image lipofuscin, an intracellular lysosomal protein that accumulates with age in human brain tissue (14) and fluoresces across the visible spectrum. Exposure times were established before the beginning of the experiment to avoid saturation of pixels for the given mRNA fluorescent grain channels. These exposure times and laser power were kept constant throughout the experiment (DAPI (100ms at 10% power), FITC (250 ms at 20% power), TRITC (250 ms at 20% power), Cy5 (600 ms at 20% power), Cy7 (500 ms at 10% power), lipofuscin (500 ms at 10% power)). Slides were coded such that the single investigator (S.J.D) was blind to diagnostic group. All subject pairs were imaged within the same 24-hour period, to minimize technical variance within a pair. For each subject, 75 sampling sites were selected to be imaged in each layer, resulting in an equivalent sampling size of 0.9075 mm^2 per layer per subject.

Image Processing

Each fluorescent channel for grains was processed using a 3D Gaussian subtraction filter in MATLAB by calculating a difference of Gaussians using sigma values of 0.7 and 2. Within SlideBook, an average z-projection algorithm was used to generate a 2D representation of the 3D image stack. To avoid inadvertently counting lipofuscin objects as grain objects, the signal in the lipofuscin channel was subtracted from grain channels of interest using channel math within SlideBook, with the exception of SOX6 (780) as the lipofuscin signal in the near-infrared channel was weak or nonexistent. Lipofuscin levels across all VGAT+/SOX6+ neurons did not differ between schizophrenia and unaffected comparison individuals ($F_{1,56}$ = 2.9, p=0.09) but lipofuscin levels were slightly higher in layer 4 in schizophrenia relative to the unaffected group within VGAT+/SOX6+ neurons (ES=+0.46, t_{89} = –2.4, p = 0.02; **Figure S1**).

To segment DAPI-labelled nuclei automatically and accurately, DAPI channel images were segmented on a pre-trained deep learning u-net in Python 3.8.5 using tensorflow packages and a keras backend (https://github.com/VolkerH/unet-nuclei). The Python script generated an RGB image which masked the DAPI nuclei, the borders of those nuclei, and the background. Within CellProfiler 4.2.0, the masked DAPI images were imported, and primary objects were designated as the pre-masked DAPI nuclei. To capture transcripts in the perinuclear cytoplasm, ‘cellular’ objects were created by expanding the perimeter of the DAPI-labeled nuclei by 2 μm until reaching the expanded perimeter of another DAPI-labeled nucleus. Grain channels were masked and size gated, and relative levels of mRNA per cell were quantified by the average

grain density per cell (grains/μm^2). Granules of lipofuscin per cell were quantified in a similar manner but were not size-gated.

Definition of Nuclei and Cells

To determine the density of grains not associated with a nucleus, grains were masked over the entirety of the image. Background grain density was determined by subtracting the grains overlapping with a DAPI-mask from the total grains over the entire image and dividing by the total image minus that total area of all DAPI nuclei. The background grain density was calculated for each subject within a given layer, providing a within-subject control for random fluctuations in background grain density or intensity. Grain density measures per cell were corrected by subtracting the background grain density quantified in the neuropil.

Assignment of nuclei that specifically expressed a given transcript was determined based on the density of grains within the boundaries of a masked nucleus. VGAT and SOX6 signals were highly localized to the nucleus, resulting in minimal background grain density (**Figure 1**). We used a relatively high threshold for designating a nucleus as VGAT+ or SOX6+, setting the threshold to 7X the background grain density for a given cell to minimize potential false positives, based on previous *in situ* studies showing high sensitivity and specificity for nuclei with this threshold (9). Because the likelihood of a false-positive identification for SST+ and PV+ cells was lower given the requirement of both VGAT+/SOX6+ identification, 4X background grain density was utilized for SST+ and PV+ cells and quantified over the ‘cellular’ object, defined as the area including a 2 μm perimeter around each nucleus, to include cytoplasmic SST and PV mRNA signal. The requirement for multiple mRNA markers co-

expressed in the same nuclei minimizes the likelihood of false positives and makes it more likely that a true difference in neuron density could be detected if one existed. Using these criteria, relatively few nuclei (<1.0% of all nuclei across subjects) were designated as VGAT+/SOX6+/SST+/PV+ **(Figure S2**); these cells were excluded from the final analysis.

Small nuclei, which might be either a glial nucleus or a fragment of a larger nucleus in a different plane of the z-axis, with a cross-sectional area less than 40 μm^2 were eliminated from the analysis. We also excluded nuclei that were located at the border of the image or not fully within the frame of view by excluding nuclei whose XY centers were located within 12 μm of the edge. This boundary was set based on the radius (center) of the largest cross-sectional area of a VGAT+ nucleus in the current study, found to be 469 μm^2.

Statistical Analysis for Comorbid Factors in Schizophrenia

In the model used to compute the BF_{10} value, the true standardized difference is assumed to be 0 under the null hypothesis and follow the Cauchy distribution under the alternative. The prior is described by a Cauchy distribution with a width parameter of 1. We selected a relatively wide prior for the BF values given the large effect sizes of SST (ES = –1.87) and PV (ES = –1.97) for this subset of subjects with schizophrenia and their matched unaffected comparison pairs selected from a larger study (15). We believe that the standard Cauchy prior scale value of 0.707, which translates to an 80% likelihood that the effect size is between –2 and 2, was too narrow given the higher likelihood that the effect size was closer to –2 based on this cohort. However, the results of the Bayesian analysis using the selected prior scale (scale = 1), a narrower prior

distribution (scale = 0.707), and a wider prior distribution (scale = 1.41) are provided in **Table S3** for each of the dependent measures.

To assess the influence of certain comorbid factors in SST and PV levels per neuron in schizophrenia, ANCOVAs were conducted using the same covariate factors as in the main analyses and the comorbid factor in each instance as the main effect. The comorbid factors analyses were conducted separately in each layer. P-values shown in the figure are corrected using the Benjamini-Hochberg procedure for multiple comparisons across comorbid factors, controlling for a 5% false discovery rate (16, 17). Comorbid analyses were only conducted in instances where there was a significant diagnosis effect observed in the main analysis.

Supplemental Tables S1–S3 and Figures S1–S7 are provided in a separate document.

Supplemental Figure Legends

Figure S1. Density of lipofuscin granules per VGAT+/SOX6+ neuron in layers 2 and 4 of the DLPFC in unaffected comparison (UC) and schizophrenia (SZ) individuals. **(A)** Boxplots of the median, quartile, and 95% range of UC and SZ for VGAT mRNA expression per VGAT+/SOX6+ neuron. Within the boxplots, values for effect size (ES), the posthoc between-group comparison p-value, and the Bayes' Factor (BF_{10}) in favor of the alternate hypothesis are shown. Bolded BF value indicates strong evidence for the null hypothesis. **(B)** Lipofuscin granule density per VGAT+/SOX6+ neuron shown as individual subject data as unity plots. In these plots, individual points represent a subject pair, and the x-axis shows the value for the unaffected individual and y-axis shows the value for the individual with schizophrenia. Colors indicate the layer for which the data are shown. Points below the line indicate a lower value in the individual with schizophrenia relative to their matched unaffected comparison individual.

Figure S2. Classification of each VGAT+/SOX6+ cell based on the expression of SST (x-axis) and PV (y-axis) mRNA levels. On the left are the values for the unaffected comparison (UC) individuals and on the right are the values for the schizophrenia (SZ) individuals in layers 2 (top panels) and 4 (bottom panels). Color indicates the classification of each VGAT+/SOX6+ cell as an SST+ or PV+ neuron, a VGAT+/SOX6+/SST+/PV+ (labeled dual positive here and were ultimately excluded from the analysis), and VGAT+/SOX6+ neurons without either SST or PV signal. The

number of neurons classified into each group is shown at the top right of each panel across all unaffected (n = 29) and schizophrenia (n = 29) individuals.

Figure S3. Histograms for individual cell data across layers. **(A)** SST levels per SST+ neuron in both layers 2 and 4 in unaffected comparison (UC) and schizophrenia (SZ). Counts are the number of cells in each category, and colors indicate the diagnostic group. **(B)** PV levels per PV+ neuron in both layers 2 and 4 in UC and SZ individuals.

Figure S4. Correlation of SST and PV measures of grain density per neuron and the density of neurons in the current study with the previous expression ratios obtained from quantitative PCR of total gray matter in the same individuals (15). **(A)** Correlation of SST mRNA per SST+ neuron, indexed by grain density per SST+ neuron averaged across layers 2 and 4 (y-axis) and the expression ratio of SST in the DLPFC total gray matter by qPCR. Each point is an individual subject, and the colors indicate the diagnosis. **(B)** Correlation of the neuron density of SST+ neurons averaged between layers 2 and 4 (y-axis) and the expression ratio of SST in the DLPFC total gray matter by qPCR (x-axis). **(C)** Correlation of PV mRNA per PV+ neuron in layer 4 (y-axis) and PV expression ratio in total gray matter (x-axis). **(D)** Correlation of the neuron density of PV+ neurons averaged between layers 2 and 4 (y-axis) and the expression ratio of SST in the total gray matter (x-axis). Pearson correlation coefficients in all panels are shown for the entire cohort.

Figure S5. Levels of VGAT and SOX6 mRNA per VGAT+/SOX6+ neuron in layers 2 and 4 of the DLPFC in unaffected comparison (UC) and schizophrenia (SZ) individuals. **(A)** Boxplots of the median, quartile, and 95% range of unaffected comparison (UC) and schizophrenia (SZ) for VGAT mRNA expression per VGAT+/SOX6+ neuron. Within the boxplots, values for effect size (ES), the posthoc between-group comparison p-value, and the Bayes' Factor (BF_{10}) in favor of the alternate hypothesis are shown. Bolded BF value indicates strong evidence for the null hypothesis. **(B)** VGAT levels per VGAT+/SOX6+ neuron shown as individual subject data as unity plots. In these plots, individual points represent a subject pair, and the x-axis shows the value for the unaffected individual and y-axis shows the value for the individual with schizophrenia. Colors indicate the layer for which the data are shown. Points below the line indicate a lower value in the individual with schizophrenia relative to their matched unaffected comparison individual. **(C)** Boxplots of the median, quartile, and 95% range of UC and SZ for SOX6 mRNA expression per VGAT+/SOX6+ neuron. **(D)** Unity plot of the individual subject data for levels of SOX6 per VGAT+/SOX6+ neuron. In all graphs, data are shown for 29 subject pairs in each layer.

Figure S6. Comparison of certain comorbid factors on SST levels per positive neuron in layer 2 (top panel) and 4 (bottom panel) in individuals with schizophrenia. P-values shown are corrected for multiple comparisons using false discovery rate of 0.05 across comorbid factors. Values at the bottom indicate the number of schizophrenia subjects with or without a certain comorbid feature. Two individuals with SZ had unknown tobacco use at time of death. Each point represents an individual SZ subject, and

boxplots show the median, quartile, and 95% range. AUD = alcohol use disorder, BZ = benzodiazepines, AEDs = antiepileptic drugs, SA = schizoaffective, SUD = substance use disorder (including opioids, cocaine, and sedatives/hallucinogens).

Figure S7. Comparison of certain comorbid factors on PV levels per positive neuron in layer 4 in individuals with schizophrenia. P-values shown are corrected for multiple comparisons using false discovery rate of 0.05 across comorbid factors. Values at the bottom indicate the number of schizophrenia subjects with or without a certain comorbid feature. Two individuals with SZ had unknown tobacco use at time of death. Each point represents an individual SZ subject, and boxplots show the median, quartile, and 95% range. AUD = alcohol use disorder, BZ = benzodiazepines, AEDs = antiepileptic drugs, SA = schizoaffective, SUD = substance use disorder (including opioids, cocaine, and sedatives/hallucinogens).

REFERENCES

1. Fung SJ, Sivagnanasundaram S, Weickert CS: Lack of change in markers of presynaptic terminal abundance alongside subtle reductions in markers of presynaptic terminal plasticity in prefrontal cortex of schizophrenia patients. Biol Psychiatry 2011;69:71–79
2. Hoftman GD, Volk DW, Bazmi HH, Li S, Sampson AR, Lewis DA: Altered cortical expression of GABA-related genes in schizophrenia: illness progression vs developmental disturbance. Schizophr Bull 2015;41:180–191
3. Azim E, Jabaudon D, Fame RM, Macklis JD: SOX6 controls dorsal progenitor identity and interneuron diversity during neocortical development. Nature Neuroscience 2009;12:1238–1247
4. Batista-Brito R, Rossignol E, Hjerling-Leffler J, Denaxa M, Wegner M, Lefebvre V, Pachnis V, Fishell G: The cell-intrinsic requirement of Sox6 for cortical interneuron development. Neuron 2009;63:466–481
5. Ma T, Wang C, Wang L, Zhou X, Tian M, Zhang Q, Zhang Y, Li J, Liu Z, Cai Y, Liu F, You Y, Chen C, Campbell K, Song H, Ma L, Rubenstein JL, Yang Z: Subcortical

origins of human and monkey neocortical interneurons. Nat Neurosci 2013;16:1588–1597

6. Volk DW, Matsubara T, Li S, Sengupta EJ, Georgiev D, Minabe Y, Sampson A, Hashimoto T, Lewis DA: Deficits in transcriptional regulators of cortical parvalbumin neurons in schizophrenia. Am J Psychiatry 2012;169:1082–1091
7. Volk DW, Edelson JR, Lewis DA: Cortical inhibitory neuron disturbances in schizophrenia: Role of the ontogenetic transcription factor Lhx6. Schizophrenia Bulletin 2014;40:1053–1061
8. DeFelipe J: Neocortical neuronal diversity: chemical heterogeneity revealed by colocalization studies of classic neurotransmitters, neuropeptides, calcium-binding proteins, and cell surface molecules. Cereb Cortex 1993;3:273–289
9. Morris HM, Hashimoto T, Lewis DA: Alterations in somatostatin mRNA expression in the dorsolateral prefrontal cortex of subjects with schizophrenia or schizoaffective disorder. Cereb Cortex 2008;18:1575–1587
10. Hashimoto T, Volk DW, Eggan SM, Mirnics K, Pierri JN, Sun Z, Sampson AR, Lewis DA: Gene expression deficits in a subclass of GABA neurons in the prefrontal cortex of subjects with schizophrenia. J Neurosci 2003;23:6315–6326
11. Dienel SJ, Ciesielski AJ, Bazmi HH, Profozich EA, Fish KN, Lewis DA: Distinct Laminar and Cellular Patterns of GABA Neuron Transcript Expression in Monkey Prefrontal and Visual Cortices. Cereb Cortex 2021;31:2345–2363
12. Fish KN, Rocco BR, Lewis DA: Laminar Distribution of Subsets of GABAergic Axon Terminals in Human Prefrontal Cortex. Front Neuroanat 2018;12:9
13. Rocco BR, Lewis DA, Fish KN: Markedly Lower Glutamic Acid Decarboxylase 67 Protein Levels in a Subset of Boutons in Schizophrenia. Biol Psychiatry 2016;79:1006–1015
14. Benavides SH, Monserrat AJ, Fariña S, Porta EA: Sequential histochemical studies of neuronal lipofuscin in human cerebral cortex from the first to the ninth decade of life. Arch Gerontol Geriatr 2002;34:219–231
15. Volk DW, Sampson AR, Zhang Y, Edelson JR, Lewis DA: Cortical GABA markers identify a molecular subtype of psychotic and bipolar disorders. Psychol Med 2016;46:2501–2512
16. Kassambara A: rstatix: Pipe-Friendly Framework for Basic Statistical Tests. 2021. R package version 0.7.0.
17. Benjamini Y, Hochberg Y: Controlling the False Discovery Rate: A Practical and Powerful Approach to Multiple Testing. Journal of the Royal Statistical Society Series B (Methodological) 1995;57:289–300

Table S1. Demographic and tissue characteristics of human postmortem samples.

Unaffected Comparison Individuals														Schizophrenia Individuals															
Pair	Case	Sex	Race	Age (yr)	BMI	PMI (hr)	pH[a]	RIN	Tissue Storage Time (mo)[b]	Medications ATOD[c]	Tobacco ATOD	Manner of Death	Cause of Death	Pair	Case	DSM-IV Schizophrenia Diagnosis ATOD	Duration of Schizophrenia Diagnosis (yr)	DSM-IV Co-Morbid Substance Use Diagnosis ATOD	Sex	Race	Age (yr)	BMI	PMI (hr)	pH[a]	RIN	Tissue Storage Time (mo)[b]	Medications ATOD[c]	Tobacco ATOD	Manner of Death	Cause of Death
1	1406	M	B	27	34.9	14.6	6.3	8.3	162.2	N	Y	Natural	Peritonitis	1	547	Schizoaffective Disorder	9	None	M	B	27	U	16.5	6.9	7.4	301.0	B C D L O P	U	Accidental	Heat Stroke
2	700	M	W	42	U	26.1	7.1	8.7	282.1	N	U	Natural	Cardiovascular Disease	2	539	Schizoaffective Disorder	31	None	M	W	50	26.4	40.9	6.9	8.1	306.6	C D O P	Y	Undetermined	Combined Drug Overdose
3	988	M	W	82	29.6	22.5	6.7	8.4	273.9	O	N	Accidental	Blunt Force Trauma	3	621	Undifferentiated Schizophrenia	55	None	M	W	83	22.6	15.6	7.2	8.7	254.8	O	U	Accidental	Asphyxiation
4	806	M	W	57	28.0	23.8	7.0	7.8	278.0	O	N	Natural	Pulmonary Embolism	4	665	Paranoid Schizophrenia	32	Alcohol Dependence	M	B	59	26.3	28.0	7.0	9.2	302.2	D O P	Y	Natural	Intestinal Hemorrhage
5	852	M	W	54	34.4	8.2	6.8	9.1	224.8	N	Y	Natural	Cardiac Tamponade	5	781	Schizoaffective Disorder	15	None	M	B	52	21.1	8.0	6.7	7.7	288.4	D O P	Y	Accidental	Peritonitis
6	987^	F	W	65	26.5	21.6	6.7	9.1	249.3	O	N	Natural	Cardiovascular Disease	6	802	Schizoaffective Disorder	43	Alcohol Dependence	F	W	63	25.2	28.9	7.0	9.2	264.2	C O P	Y	Natural	Cardiovascular Disease
7	727	M	B	19	25.6	7.0	7.0	9.2	224.8	N	N	Accidental	Blunt Force Trauma	7	829	Schizoaffective Disorder	5	Alcohol Dependence	M	W	25	24.2	5.0	6.8	9.3	260.1	B C	Y	Suicide	Salicylate Overdose
8	1374	M	W	43	41.0	21.7	6.6	7.2	258.0	O	Y	Natural	Cardiovascular Disease	8	904	Schizoaffective Disorder	8	None	M	W	33	38.4	28.0	6.3	7.1	238.0	C O P	Y	Natural	Pneumonia
9	818	F	W	67	37.8	23.5	7.1	8.4	248.1	O	N	Accidental	Anaphylaxis	9	917	Undifferentiated Schizophrenia	50	None	F	W	71	25.5	23.8	7.1	7.0	234.6	O P	Y	Natural	Cardiovascular Disease
10	857	M	W	48	21.7	16.2	6.7	8.9	273.0	N	Y	Natural	Cardiovascular Disease	10	930	Disorganized Schizophrenia	28	None	M	W	47	34.6	15.3	6.3	8.2	234.0	C O	Y	Natural	Cardiovascular Disease
11	739	M	W	40	19.2	15.8	6.7	8.4	209.1	N	Y	Natural	Cardiovascular Disease	11	933	Disorganized Schizophrenia	22	None	M	W	44	45.6	8.3	6.1	8.1	200.5	C D O P	N	Natural	Myocarditis
12	10003	M	W	49	29.2	21.2	6.5	8.4	174.1	N	N	Accidental	Blunt Force Trauma	12	1088	Undifferentiated Schizophrenia	24	Alcohol Dependence; Cannabis Abuse	M	W	49	27.1	21.5	6.4	8.1	200.7	D O P	Y	Accidental	Combined Drug Overdose
13	1122	M	W	55	29.2	15.4	6.5	8.9	205.5	O	Y	Natural	Cardiac Tamponade	13	1105	Schizoaffective Disorder	5	None	M	W	53	30.3	7.9	6.1	8.9	207.6	P	Y	Natural	Cardiovascular Disease
14	1336	M	W	65	27.8	18.4	6.7	8.0	184.6	O	Y	Natural	Cardiac Tamponade	14	1173	Disorganized Schizophrenia	33	None	M	W	62	22.9	22.9	6.3	7.7	198.9	O P	Y	Natural	Cardiovascular Disease
15	1092	F	B	40	39.3	16.6	6.7	8.0	226.9	O	N	Natural	Mitral Valve Prolapse	15	1178	Schizoaffective Disorder	11	None	F	B	37	31.7	18.9	6.1	8.4	194.1	B P	Y	Natural	Pulmonary Embolism
16	1284	M	W	55	25.2	6.4	6.8	8.7	198.0	N	Y	Natural	Cardiovascular Disease	16	1188	Undifferentiated Schizophrenia	33	None	M	W	58	17.3	7.7	6.1	8.4	209.5	C O P	Y	Natural	Cardiovascular Disease
17	970	M	W	42	28.6	25.9	6.4	7.2	190.1	N	Y	Natural	Cardiovascular Disease	17	1222	Undifferentiated Schizophrenia	16	Alcohol Abuse	M	W	32	31.8	30.8	6.4	7.5	190.9	D P	N	Suicide	Combined Drug Overdose
18	1268	M	B	49	27.1	19.9	6.9	7.9	176.6	O	N	Natural	Cardiovascular Disease	18	1230	Undifferentiated Schizophrenia	28	None	M	W	50	31.9	16.9	6.4	8.2	190.2	D O P	Y	Suicide	Doxepin Overdose
19	1247	F	W	58	35.9	22.7	6.2	8.4	208.1	O	N	Natural	Cardiovascular Disease	19	1240	Undifferentiated Schizophrenia	25	None	F	B	50	44.6	22.9	6.2	7.7	189.4	O P	Y	Natural	Cardiovascular Disease
20	1159	M	W	51	38.5	16.7	6.5	7.6	202.0	O	N	Natural	Cardiovascular Disease	20	1296	Undifferentiated Schizophrenia	35	None	M	W	48	16.7	7.8	6.3	7.3	182.3	D O P	Y	Natural	Pneumonia
21	1326	M	W	58	32.1	16.4	6.7	8.0	176.2	O	N	Natural	Cardiovascular Disease	21	1314	Undifferentiated Schizophrenia	33	None	M	W	50	22.1	11.0	6.6	7.2	178.8	C D O P	N	Natural	Cardiovascular Disease
22	1466	F	B	64	27.1	20.0	6.7	8.8	241.2	O	N	Accidental	Blunt Force Trauma	22	1341	Schizoaffective Disorder	30	Opioid Dependence	F	W	44	19.1	24.5	6.5	8.8	171.5	B O P	N	Accidental	Penetrating Force Trauma
23	902	M	W	60	25.2	23.6	6.6	7.7	169.4	N	Y	Natural	Cardiovascular Disease	23	1361	Schizoaffective Disorder	47	None	M	W	63	26.7	23.2	6.4	7.7	241.2	C O P	Y	Natural	Cardiomyopathy
24	1792	F	W	36	21.0	28.1	6.4	7.5	186.9	O	Y	Natural	Pulmonary Embolism	24	1506	Schizoaffective Disorder	29	Alcohol Dependence	F	W	47	48.7	14.1	6.6	7.5	192.5	D O P	Y	Accidental	Combined Drug Overdose
25	1270	F	W	73	24.6	19.7	6.7	7.7	151.8	O	N	Accidental	Blunt Force Trauma	25	1579	Schizoaffective Disorder	44	Alcohol Dependence; Sedative or Hypnotic or Anxiolytic Dependence	F	W	69	22.9	16.1	6.6	7.7	173.4	B O P	Y	Natural	Cardiovascular Disease
26	1583	M	W	58	23.2	19.1	6.7	8.2	94.0	N	Y	Accidental	Blunt Force Trauma	26	1686	Paranoid Schizophrenia	36	None	M	B	56	28.5	14.1	6.2	8.3	144.8	B D O P	Y	Natural	Cardiovascular Disease
27	1384	M	W	67	26.5	21.9	6.6	7.0	186.6	O	Y	Natural	Cardiovascular Disease	27	1712	Schizoaffective Disorder	45	Sedative or Hypnotic or Anxiolytic Dependence	M	W	63	33.1	15.1	6.1	7.1	130.0	C D O P	N	Natural	Cardiovascular Disease
28	1558	M	W	54	20.6	24.4	6.8	7.7	129.4	O	N	Natural	Cardiovascular Disease	28	1734	Undifferentiated Schizophrenia	32	Cannabis Dependence	M	W	54	22.8	28.6	6.1	7.7	112.7	O P	Y	Natural	Pneumonia
29	1324	M	W	43	30.9	22.3	6.8	7.3	167.3	N	N	Natural	Aortic Dissection	29	10020	Paranoid Schizophrenia	20	Alcohol Abuse; Other/Unknown Substance Abuse	M	W	38	19.8	28.8	6.5	7.4	106.3	C D P	Y	Suicide	Salicylate Overdose
30	1099	F	W	24	18.2	9.1	6.5	8.6	134.2	O	Y	Natural	Cardiomyopathy	30	10023	Disorganized Schizophrenia	10	None	F	B	25	32.8	20.1	6.5	7.4	102.6	B D P	N	Suicide	Drowning
	Mean			**51.5**	**28.6**	**19.0**	**6.7**	**8.2**	**202.9**						**Mean**		**27.8**				**50.1**	**28.3**	**19.0**	**6.5**	**8.0**	**206.7**				
	Standard Deviation			**14.3**	**6.1**	**5.7**	**0.2**	**0.6**	**47.0**						**Standard Deviation**		**13.7**				**13.8**	**8.2**	**8.6**	**0.3**	**0.7**	**56.1**				

Footnotes:

[a]Reported value is the mean of prefrontal and cerebellar or occipital pH values. Case 818 is the exception, with only the prefrontal pH value reported.

[b]Stored at -80C

[c]Medications at time of death: B, benzodiazepines; C, anticonvulsants; D, antidepressants; L, lithium; N, no medications; O, other medication(s); P, antipsychotic; U, unknown

^987: Posttraumatic Stress Disorder in remission for 39 years

Abbreviations:

yr, years; PMI, postmortem interval (hours); RIN, RNA integrity number; mo, months; ATOD, at time of death; F, female; M, male; B, black; W, white; Y, yes; N, no; U, unknown

Table S2. Reagents Used

Reagent	Vendor	Reference/Catalog	Lot
Hs-SOX6 - C1	ACDbio	524791	20058B
Hs-SLC32A1 - C2	ACDbio	415681 - C2	20059C
Hs-SST - C3	ACDbio	310591 - C3	20059C
Hs-PVALB - C4	ACDbio	422181 - C4	20059C
RNAscope v2 kit	ACDbio	323110	2007958
RNAscope Ancillary Kit	ACDbio	323120	2007469
H_2O_2	ACDbio	322335	2008735
1X Plus Amplificiation Diluent	Akoya Biosciences	FP1498	191213005
Opal 520	Akoya Biosciences	OP001001	20194101
Opal 570	Akoya Biosciences	OP-001003	20193901
TSA Cy5	Akoya Biosciences	FP1171	2620021
Opal 780	Akoya Biosciences	OP-001008	20194201
TSA DIG	Akoya Biosciences	OP-001007	20200102
Prolong Diamond Antifade Mountant	ThermoFisher	P36970	2168848A

Table S3. Table of Each Measure, Associated Effect Sizes, and Confidence Intervals, Test Statistics, and Bayes' Factors

Comparison (SZ – UC)	Cell Type	Figure Reference	Layer	Effect Size (ES)	95% CI of ES	Test Statistic	p-value	Bayes' Prior Selection		
								Default (scale = 1)	Narrower (scale = 0.707)	Wider (scale = 1.41)
SST Levels	VGAT+/SOX6+/SST+	Figure 2A & 2B	Layer 2	–1.48	[–0.89 to –2.1]	$t_{(64.5)} = 5.3$	<0.00001	2.4e4	2.1e4	2.6e4
SST Levels	VGAT+/SOX6+/SST+	Figure 2A & 2B	Layer 4	–1.64	[–1.0 to –2.3]	$t_{(64.5)} = 6.7$	<0.00001	2.3e5	1.9e5	2.5e5
SST Neuron Density	VGAT+/SOX6+/SST+	Figure 2C & 2D	Layer 2	+0.07	[+0.60 to –0.46]	$t_{(105.7)} = –0.49$	0.62	0.20	0.27	0.15
SST Neuron Density	VGAT+/SOX6+/SST+	Figure 2C & 2D	Layer 4	–0.22	[+0.31 to –0.75]	$t_{(105.7)} = 0.44$	0.66	0.27	0.36	0.20
PV Levels	VGAT+/SOX6+/PV+	Figure 3A & 3B	Layer 2	–0.23	[+0.29 to –0.76]	$t_{(78.2)} = 1.3$	0.20	0.28	0.37	0.21
PV Levels	VGAT+/SOX6+/PV+	Figure 3A & 3B	Layer 4	–1.14	[–0.58 to –1.71]	$t_{(78.2)} = 5.3$	<0.00001	3.8e2	3.6e2	3.7e2
PV Neuron Density	VGAT+/SOX6+/PV+	Figure 3C & 3D	Layer 2	+0.21	[+0.74 to –0.31]	$t_{(101.8)} = –0.11$	0.91	0.27	0.35	0.20
PV Neuron Density	VGAT+/SOX6+/PV+	Figure 3C & 3D	Layer 4	+0.17	[+0.70 to –0.35]	$t_{(101.8)} = –0.22$	0.82	0.24	0.32	0.18
VGAT+/SOX6+ Neuron Density	VGAT+/SOX6+	Figure 4A & 4B	Layer 2	+0.37	[+0.90 to –0.16]	$t_{(98.2)} = –1.8$	0.08	0.47	0.60	0.36
VGAT+/SOX6+ Neuron Density	VGAT+/SOX6+	Figure 4A & 4B	Layer 4	+0.23	[+0.80 to –0.30]	$t_{(98.2)} = –1.0$	0.32	0.28	0.37	0.21
VGAT Levels	VGAT+/SOX6+	Supp. Figure 4A & 4B	Layer 2	–0.18	[+0.08 to –0.44]	$t_{(75.4)} = 0.94$	0.35	0.26	0.36	0.19
VGAT Levels	VGAT+/SOX6+	Supp. Figure 4A & 4B	Layer 4	–0.30	[–0.03 to –0.56]	$t_{(76.0)} = 1.6$	0.12	1.1	1.5	0.82
SOX6 Levels	VGAT+/SOX6+	Supp. Figure 4C & 4D	Layer 2	+0.50	[+1.0 to –0.04]	$t_{(67.4)} = –2.0$	0.08	0.95	1.2	0.75
SOX6 Levels	VGAT+/SOX6+	Supp. Figure 4C & 4D	Layer 4	+0.13	[+0.66 to –0.40]	$t_{(67.4)} = –0.61$	0.54	0.22	0.30	0.16

Figure S1

Lipofuscin Granules in VGAT+/SOX6+ Neurons

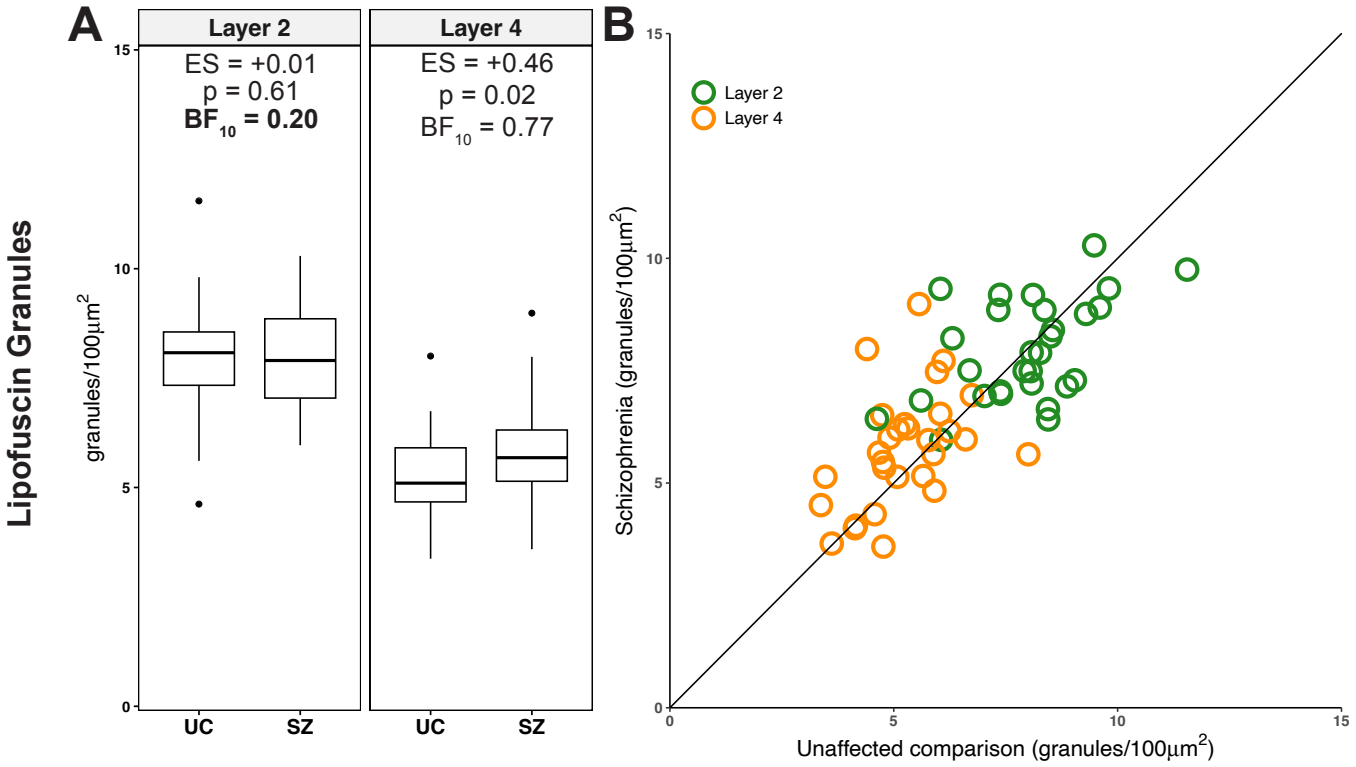

Figure S2

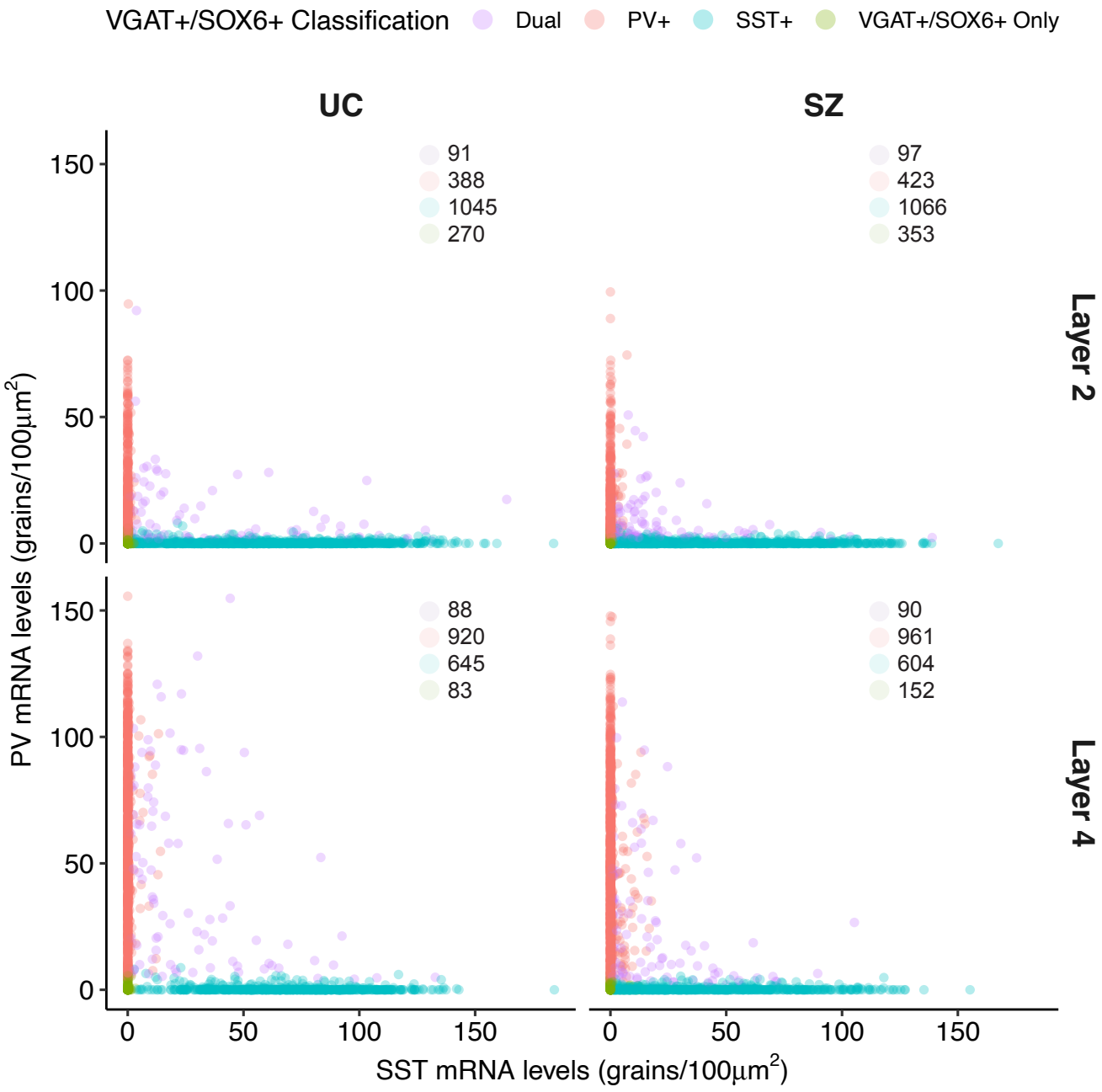
VGAT+/SOX6+ Classification
Dual
PV+
SST+
VGAT+/SOX6+ Only
UC
SZ
Layer 2
Layer 4
91
388
1045
270
97
423
1066
353
88
920
645
83
90
961
604
152
PV mRNA levels (grains/100µm²)
SST mRNA levels (grains/100µm²)
0
50
100
150

Figure S3

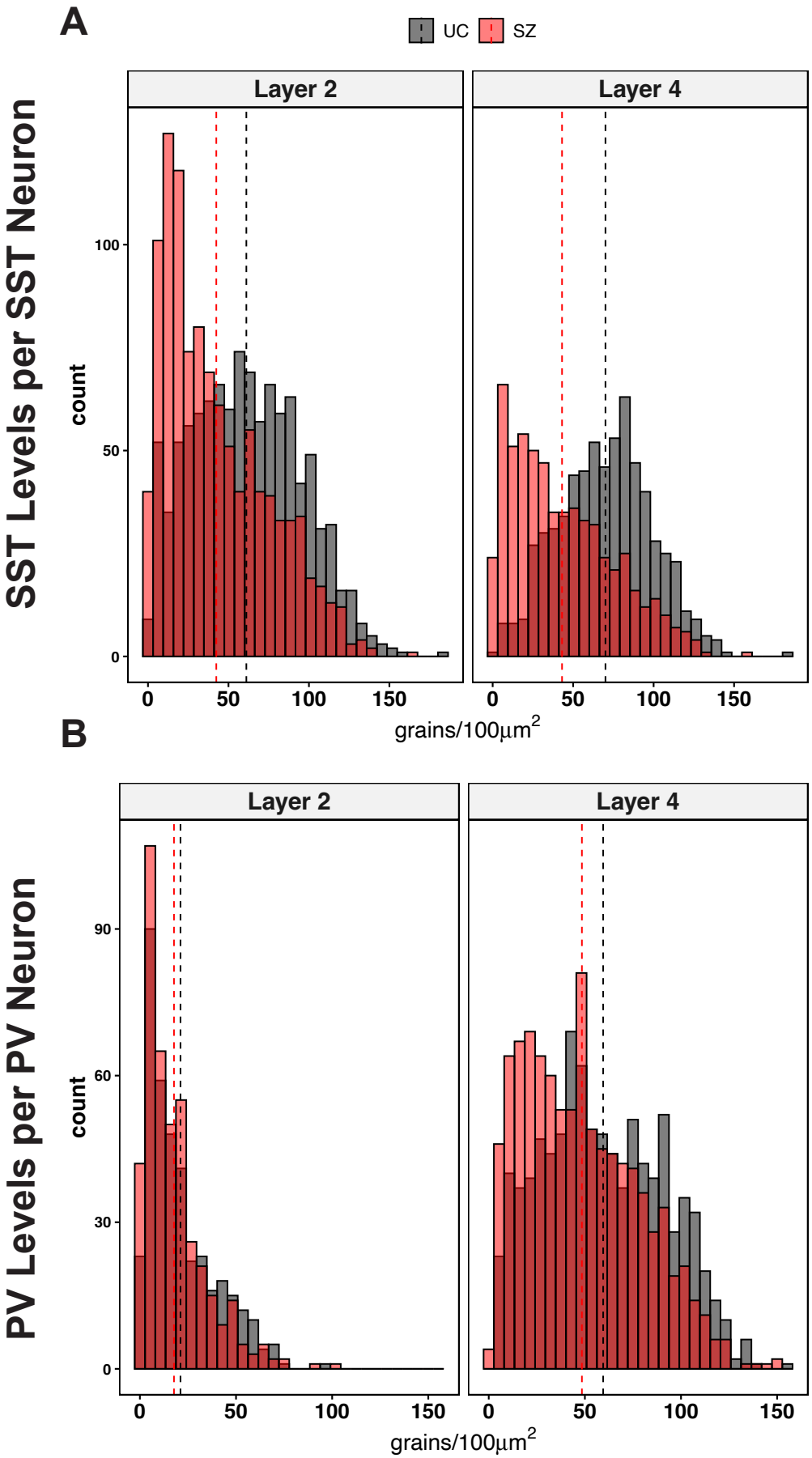
A
UC
SZ
Layer 2
Layer 4
SST Levels per SST Neuron
count
100
50
0
0
50
100
150
grains/100µm2
B
Layer 2
Layer 4
PV Levels per PV Neuron
count
90
60
30
0
0
50
100
150
grains/100µm2

Figure S4

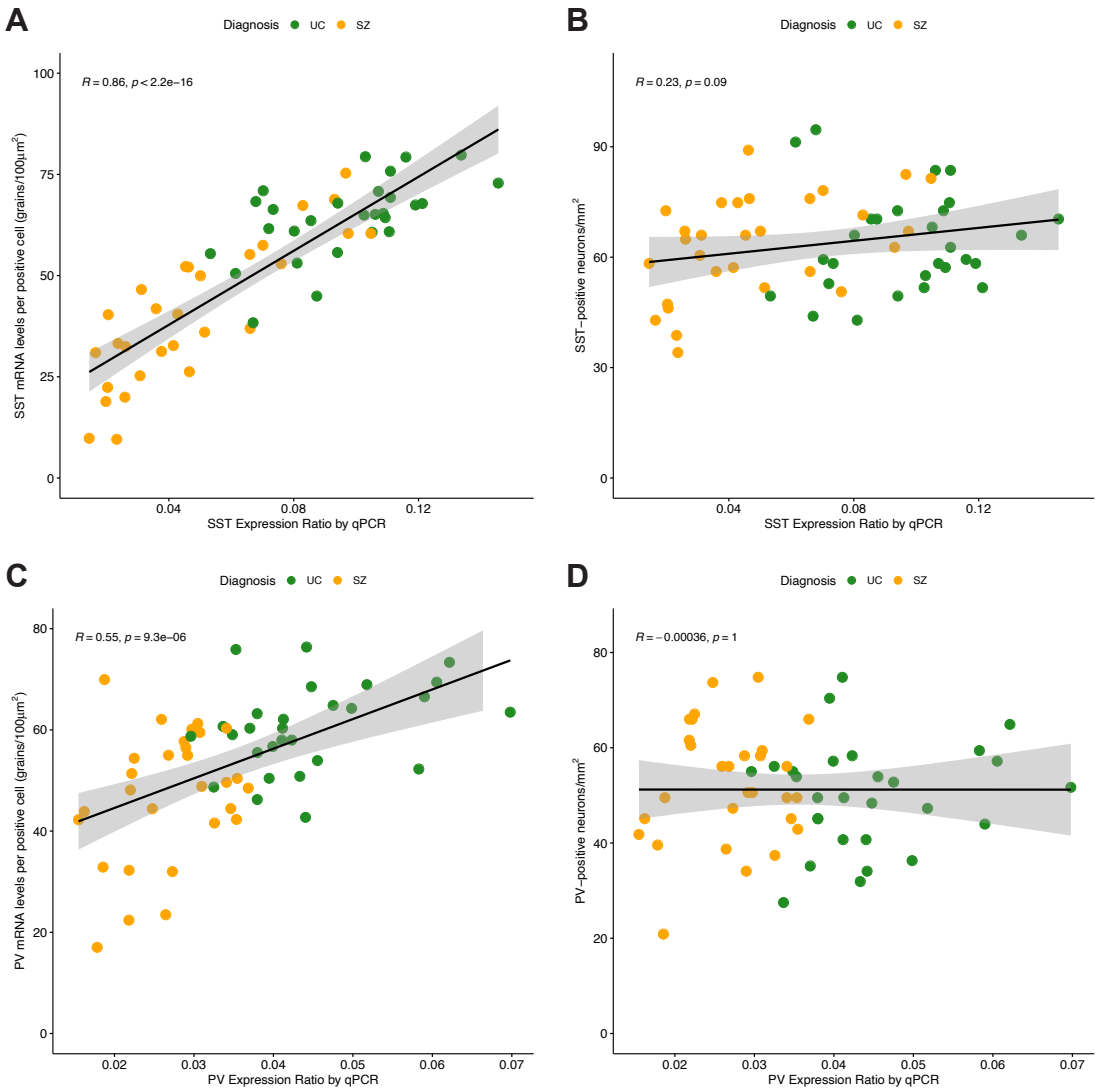
A
Diagnosis UC SZ
R = 0.86, p < 2.2e−16
SST mRNA levels per positive cell (grains/100μm²)
SST Expression Ratio by qPCR
B
Diagnosis UC SZ
R = 0.23, p = 0.09
SST−positive neurons/mm²
SST Expression Ratio by qPCR
C
Diagnosis UC SZ
R = 0.55, p = 9.3e−06
PV mRNA levels per positive cell (grains/100μm²)
PV Expression Ratio by qPCR
D
Diagnosis UC SZ
R = −0.00036, p = 1
PV−positive neurons/mm²
PV Expression Ratio by qPCR

Figure S5

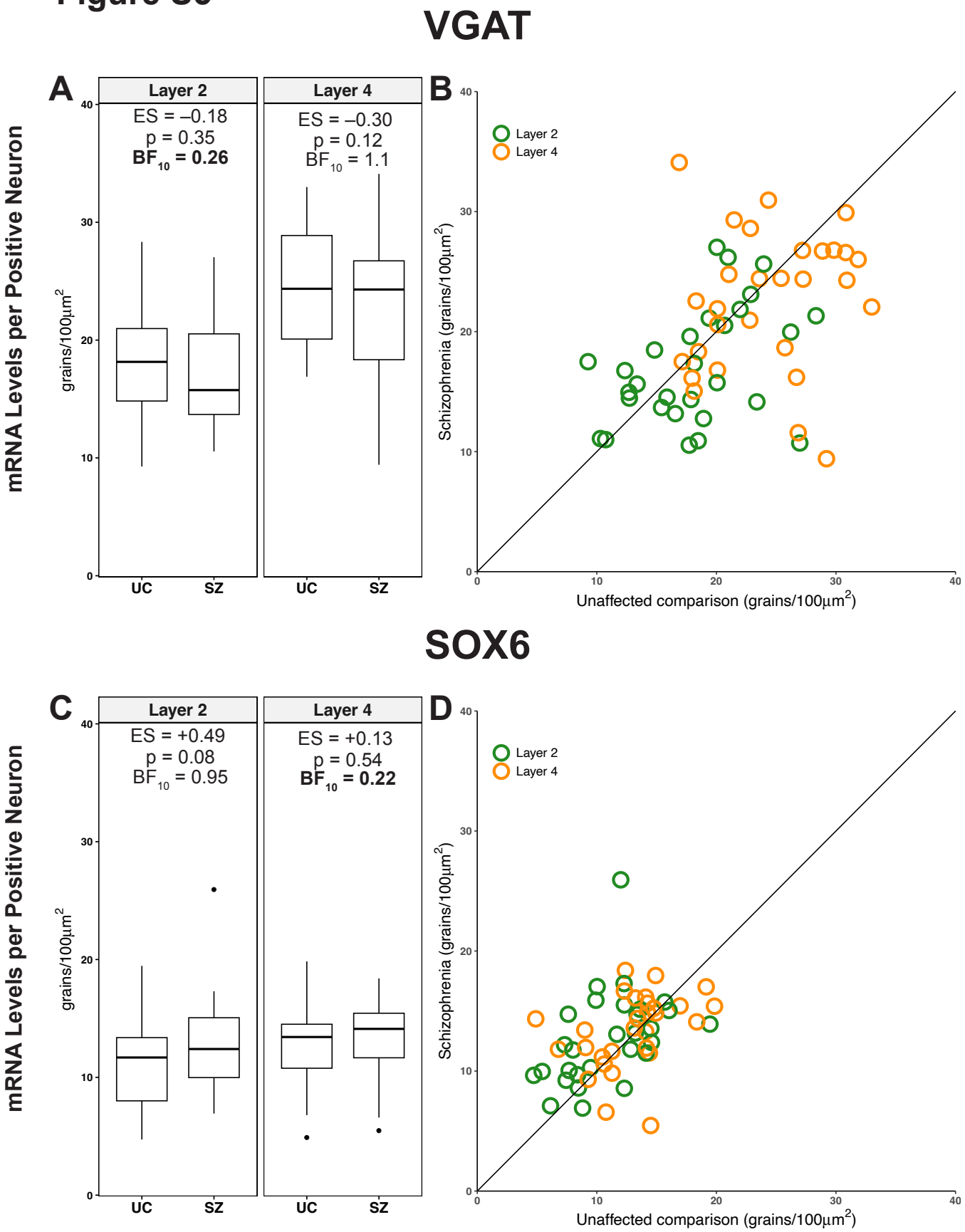
VGAT
A
Layer 2
Layer 4
ES = –0.18
p = 0.35
BF10 = 0.26
ES = –0.30
p = 0.12
BF10 = 1.1
mRNA Levels per Positive Neuron
grains/100µm2
UC
SZ
B
Layer 2
Layer 4
Schizophrenia (grains/100µm2)
Unaffected comparison (grains/100µm2)
SOX6
C
Layer 2
Layer 4
ES = +0.49
p = 0.08
BF10 = 0.95
ES = +0.13
p = 0.54
BF10 = 0.22
mRNA Levels per Positive Neuron
grains/100µm2
UC
SZ
D
Layer 2
Layer 4
Schizophrenia (grains/100µm2)
Unaffected comparison (grains/100µm2)

Figure S6

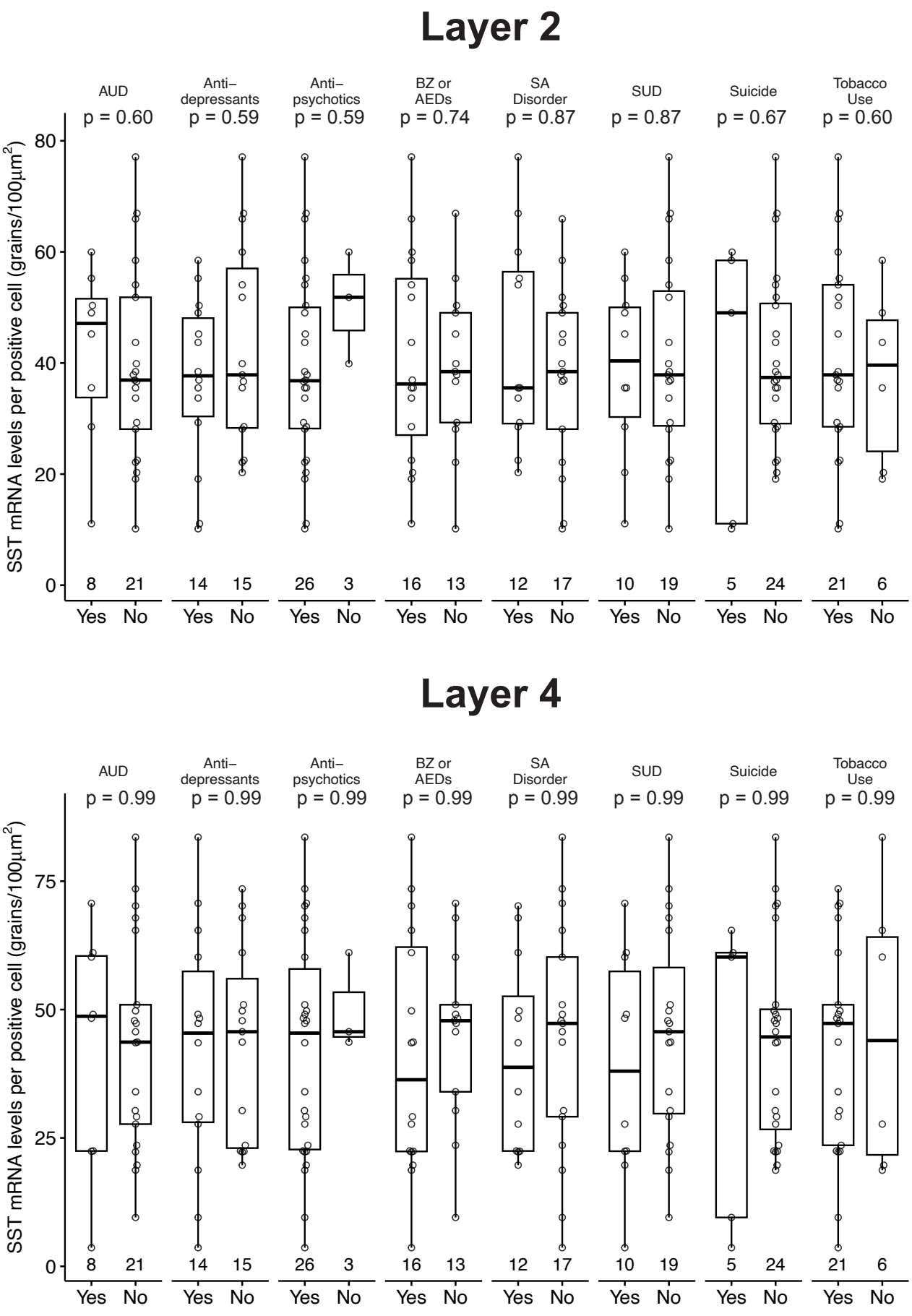
Layer 2
AUD
Anti–depressants
Anti–psychotics
BZ or AEDs
SA Disorder
SUD
Suicide
Tobacco Use
p = 0.60
p = 0.59
p = 0.59
p = 0.74
p = 0.87
p = 0.87
p = 0.67
p = 0.60
SST mRNA levels per positive cell (grains/100µm²)
0
20
40
60
80
8 21 14 15 26 3 16 13 12 17 10 19 5 24 21 6
Yes No
Layer 4
AUD
Anti–depressants
Anti–psychotics
BZ or AEDs
SA Disorder
SUD
Suicide
Tobacco Use
p = 0.99
p = 0.99
p = 0.99
p = 0.99
p = 0.99
p = 0.99
p = 0.99
p = 0.99
SST mRNA levels per positive cell (grains/100µm²)
0
25
50
75
8 21 14 15 26 3 16 13 12 17 10 19 5 24 21 6
Yes No

Figure S7

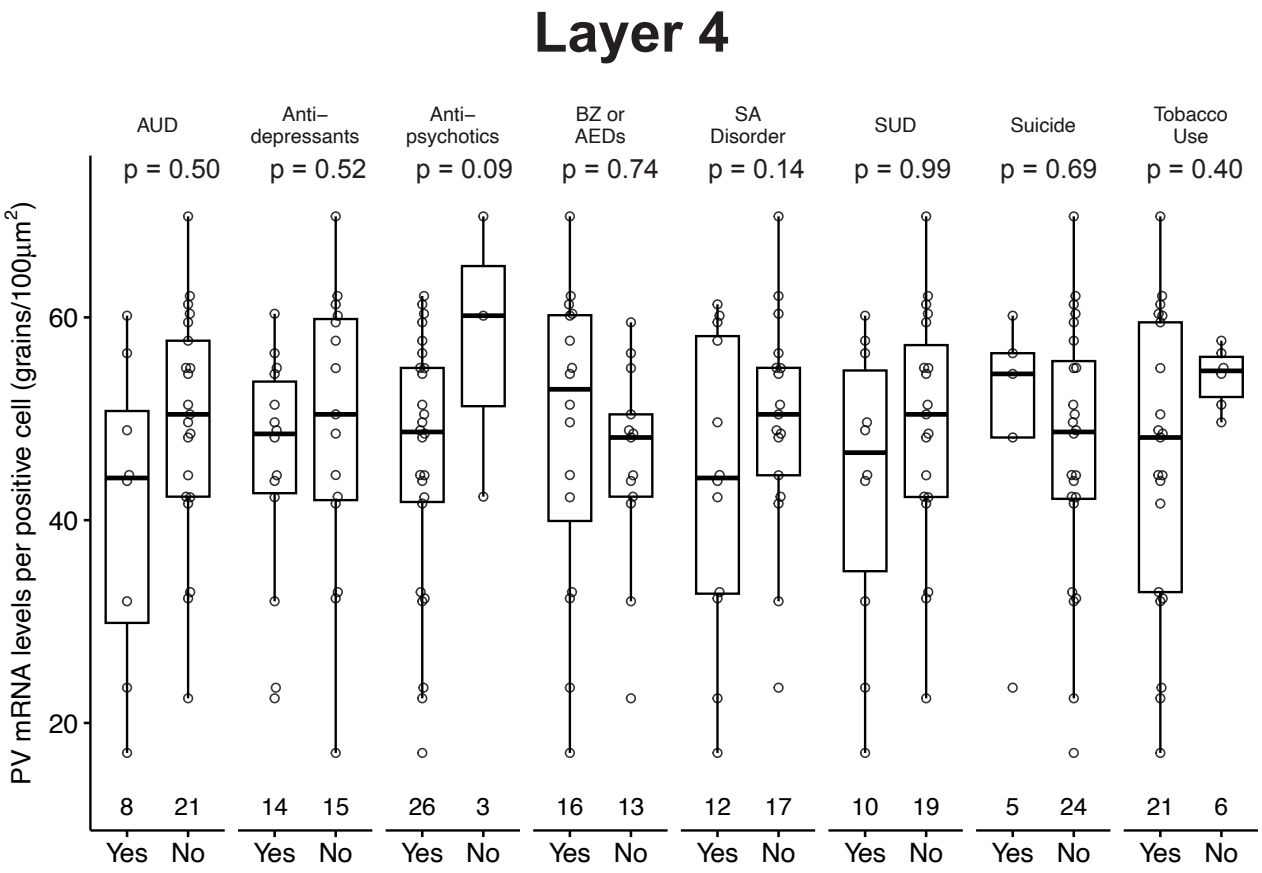
Layer 4
AUD
Anti–depressants
Anti–psychotics
BZ or AEDs
SA Disorder
SUD
Suicide
Tobacco Use
p = 0.50
p = 0.52
p = 0.09
p = 0.74
p = 0.14
p = 0.99
p = 0.69
p = 0.40
PV mRNA levels per positive cell (grains/100μm²)
60
40
20
8 21
14 15
26 3
16 13
12 17
10 19
5 24
21 6
Yes No